

Epidemic protection zones: centered on cases or based on connectivity ?

AL Rivas^{1,2}, FO Fasina³, KJ Sumption⁴, SD Smith⁵, AL Hoogesteyn⁶, JL Febles⁶, JB Hittner⁷, and DJ Perkins¹

Transbound. Emerg. Dis. (Short Comm)

¹Health Sciences Center, University of New Mexico, Albuquerque, New Mexico, USA

²College of Veterinary Medicine, North Carolina State University, Raleigh, North Carolina, USA; ³Faculty of Veterinary Science, University of Pretoria, South Africa, and Faculty of Veterinary Medicine, Utrecht University, Yaleaan, The Netherlands

⁴European FMD Commission, Food and Agricultural Organization, Rome, Italy;

⁵College of Agriculture and Life Sciences, Cornell University, Ithaca, New York, USA;

⁶Dept. of Human Ecology, CINVESTAV, Merida, Yucatan, Mexico; and ⁷Dept. of Psychology, College of Charleston, 66 George St., Charleston, South Carolina, USA.

Keywords: health geographics, protection zones, networks, connectivity, roads

Correspondence: A. L. Rivas, DVM, PhD, Center for Global Health, Health Sciences Center, Biomedical Research Facility, MSC 10.5550 –1 University of New Mexico, University of New Mexico, Albuquerque, NM 87131, USA. Tel.: 1-505-272-5016; Fax: 1-505-272-8441; E-mail:alrivas@unm.edu

Running Head: Equal-radius vs. biogeographical protection zones against epidemics

Summary (<300 words Now: 273 words)

When an exotic infectious disease invades a susceptible environment, protection zones are enforced. Historically, such zones have been shaped as circles of equal radius (ER), centered on the location of infected premises. Because the ER policy seems to assume that epidemic dissemination is driven by a similar (median) number of secondary cases generated per primary case, it does not consider other features of the infected area, such as its connectivity. Here we explored the efficacy of ER protection zones. By generating a geographically explicit scenario that mimicked an actual epidemic, we created protection zones of different geometry, comparing the cost-benefit estimates of ER protection zones to several alternatives, which considered a geographically explicit, pre-existing connecting network (CN) –the road network. The CN policy required 20% less area to be protected than the ER policy. The CN-based protection zone included a higher number of units at risk/sq km, higher length of roads, and a higher road density (km of roads/sq km) than the ER-based alternative, that is, the CN policy achieved greater benefits with 80% of the costs. The hypothesis of similar number of cases per ER circle was not substantiated: the number of units at risk per circle differed up to 4 times among ER circles. The data suggested that protection zones are likely to be less costly and more effective if they consider bio-geographical connecting structures, such as road, railroad, and/or river networks. Findings showed that even a small area (of less than 115 sq km) revealed network properties. Because invading microbes do not create connecting structures but, to survive and disseminate, depend on such networks, proactive assessment of connectivity is recommended.

Introduction (Now: 2173 words; acceptable: ~2000 w)

Equal radius (ER) circular protection zones have classically been applied to control epidemics (Thrusfield et al., 2005; Jewell et al., 2009; Lu et al., 2010; Knight-Jones et al., 2011; Thulke et al., 2011). They are geographically well-defined zones where some control measures are applied. While rapidly disseminating epidemics have been investigated under biological perspectives and/or considering the source of the epidemic (Cottam et al., 2008; Ryan et al., 2008; Lu et al. 2010), the validity of protection zones based on ER circles has not been explored (Cook et al., 2006). Such protection zones assume mean-field (homogeneous-mixed) epidemic dissemination, i.e., because all members of the population are suspected to be equally connected, the geographical location of individuals, and the interactions between the structure and the bio-geographical variables of the infected area, are ignored (Filipe and Maule, 2004; Aparicio and Pascual, 2007; Dangerfield et al., 2008).

An alternative view has proposed that disease spread is explained by network properties (those of points or nodes, connected by lines, Watts and Strogatz, 1998; Barthelemy, 2011). However, there is no consensus on what network factors should be investigated. While most studies have focused on contacts (e.g., people, animals), only a few reports have assessed connectivity, such as road networks (Rivas et al., 2003; Martinez-Lopez et al., 2009; Rivas et al. 2010).

Network properties may express Pareto's '20:80' pattern, i.e., approximately 20% of all infected sites include approximately 80% of the cases. Such pattern, if observed when geo-referenced epidemic data are analyzed, would demonstrate that mean-field based assumptions are not optimal to explain or control disease spread (Chowell et al., 2008; Andriani and McKelvey, 2009).

Network theory can be integrated with cost-benefit analysis (Rivas et al., 2004). Network constructs can evaluate whether less costly/more beneficial epidemic control measures could be generated when geographically explicit data are considered.

Here we explored whether epidemic control policy based on identical (equal radius) protection circles was empirically justified. The null hypothesis was that all circles would reveal a similar number of 'sites at risk' while the alternative was that they would differ. In addition, we asked:

- i. are circles of equal radius (ER) similar in their ability to protect?
- ii. are ER-based protection zones optimal?
- iii. what cost/benefit estimates (area of the region to be protected, density of sites at risk/sq km, road density/sq km) are associated with ER circles? and
- iv. what cost/benefit estimates are associated with an area (of any geometric shape) that considers the local connectivity?

To answer these questions, we created a bio-geographical scenario, which summarized some geographically explicit features associated with an actual epidemic, which included the boundaries of the protection zone enforced in that epidemic. Because this study did not evaluate diagnostics or control measures, the infective agent, host species, place, and time when the epidemic took place were not considered. Instead, the focus of interest was to determine cost-benefit estimates associated with protection zones. This report can be viewed as a study of a bio-geographical (geometric) structure that was summarized, which was not hypothetical. Based on geo-referenced data of past epidemics

(Supporting Materials), we reproduced the overall protection zone then applied, including some geographical features (e.g., location of sites at risk [e.g., farms] and highways of the epidemic area). Based on Xia and Levinson (2007), connectivity was described in terms of proximity, continuity, and road length: we considered the total road length included in protection zones, as well as the degree of fragmentation of the road structure (whether all highway segments were linked or not), and whether points (farms at risk) could be interconnected or not, given their distance to highways (proximity). For simplicity, we only considered major highways. Later, we determined the number of farms at risk/sq km found within the original ER protection zone, as well as its corresponding road density. Then, we empirically determined the smallest circle that (i) was close to either highways or highway intersections, and (ii) included the highest number of farms at risk. Finally, we created several polygons that included most (or all) farms at risk, and were partially (or totally) connected through road links. Findings showed that the less costly/more beneficial solution included a geographically explicit connecting network, not ER circles.

Methods

Creation of a geographically explicit epidemic scenario

The image of a geographically specific region, where a specific epidemic took place at a specific point in time ('epidemic report', described in Supporting Materials), was exported into a JPG file format. Using ArcGIS 10.1 (ESRI, Redlands, CA), the epidemic report (jpg file) was geo-referenced to the WGS 1984 Web Mercator Auxiliary Sphere projection, taking four road intersections shown on the jpg file to correspond with the same intersections reported on a BING map layer accessed from ArcGIS Online (<http://www.arcgis.com/home/>). In order to facilitate area and distance calculations, the geo-referenced image was projected into the ETRS 1989 UTM (Zone 30, North) projection. The radius of individual 'farm at risk' site areas was empirically derived from the protection zone of the epidemic report, i.e., circles of various radii were created until their segments matched the boundaries of the protection zone shown in the epidemic report. After such procedure identified 9 circles of equal radius, their corresponding centroids (sites where 'farms at risk' [n=9] were located) were calculated. The road network associated with the protection zone was digitized, including road segments located outside such zone. Buffers were created (a polygon was generated), centered on the road layer and built to encompass all 9 locations of farms at risk. An additional site location (centroid and circle #10) was digitized, which corresponded to a highway intersection located near to but outside the southeast border of the epidemic report's protection zone. A second set of buffers (a second polygon) was created by joining the additional site location (circle #10) with a polygon that not only included all farms at risk, but also road segments in a way such that a non-fragmented (continuous) road network would be generated. The original road layer, which included road segments outside the epidemic report's protection zone, was clipped to include the larger polygon described above (which included the 10th. buffer --point corresponding to the highway intersection located outside the protection zone). Areas (sq km) and distances (km) were calculated for each data layer using the 'calculate geometry' field tool provided by ArcGIS 10.1.

Statistical analysis

Because this study only analyzed a single geometric structure (assumed to represent a

single point in time), the temporal progression or transmission the epidemic was not analyzed. The Wilcoxon Signed Rank test was conducted to determine whether the median number of ‘farms at risk’ at ER circles was equal to 1 (as expected under the assumption of homogeneous epidemic dissemination over space). After extracting both the Euclidean distance between each farm at risk and the nearest road or road intersection, and the Euclidean distance between farm pairs, a Mann-Whitney test for the median was conducted to determine whether the median inter-farm distance differed from the distance between farms and roads or intersections. A Chi square goodness-of-fit test was conducted to quantify the contribution of each ER circle with farms at risk to the global Chi square value. Statistical tests were conducted in Minitab 15.

Results and Discussion

A protection zone applied to an area where an exotic microbe had been found was re-created, generating the geo-referenced data that facilitated this study (Fig. 1 and Supporting Materials). All 9 centroids derived from the 9 circles so created were assumed to be ‘farms at risk’, i.e., this study did not determine their health status (Fig. 1A).

The number of farms at risk per circle differed up to 4 times among the 9 circles (Figs. 1 B-E). The median number of farms at risk per ER circle was 2.5 (Supporting Materials). The circles that revealed the highest number of farms at risk partially overlapped, and included a highway intersection (Fig. 1F).

The overall risk density in the ER protection zone was 0.063 farms/sq km (9 farms/142.5 sq km), which corresponded to a road density of 0.22 km/sq km (32.34 km of roads/142.5 sq km, or, alternatively, to 0.278 farms at risk / km of roads (9/32.34 km). (Figs. 2A, B, respectively).

A higher density of farms at risk was observed when alternative (also circular) protection zones were created, which were centered on the only highway intersection found within the original protection zone. By creating circles of various radii, three densities were calculated, which ranged between 0.144 farms at risk/sq km (4/27.75, smallest [2.9-km radius] circle) and 0.056 (6/106.37 cases/sq km, largest [5.7-km radius] circle, which partially fell outside the boundaries of the original protection zone). The road density, in the smallest circle centered on the road intersection, was 0.429 km/sq km (11.91 km/ 27.75 sq km, Fig. 2C). Therefore, in the smallest of these circles centered on the only highway intersection, 44.4% (4/9) of all farms at risk were located within 19.5 % of the total area (27.75/142.5 sq km), which indicated that, if proximity (≤ 2.9 -km) to a highway intersection was considered, the number of farms at risk was almost 2.3 times (44.4/19.5) higher than expected under the hypothesis of homogeneous dissemination, and that structure was associated with an almost twice higher road density.

If, instead, the smallest polygon that included all farms at risk had been considered, its density would have been 0.132 farms at risk/sq km (7/52.86), but only if continuous road segments had been considered. Such polygon captured 77.7% (7/9) of the farms at risk, which were located within 37.09% (52.86/142.5 sq km) of the whole area –more than twice (2.09 or 77.7/37.09) the density expected under the homogeneous dissemination hypothesis. While this alternative displayed a density of farms at risk similar to that of the smallest circle centered on a road intersection and a much higher number of farms at risks than the value observed in the smallest circle centered on the intersection (77.7% vs. 44.4%), this polygon did not connect all farms at risk through a

geographically explicit and continuous road network. Because one road segment was not included in the polygon, two farms at risk appeared to lack connectivity (Fig. 2D).

If, instead, the surface of the region to be protected was expanded to include a highway intersection observed outside the south-east border of the original protection zone, all farms at risk (100% or 9/9) would be included within a polygon that revealed a continuous road structure (Fig. 2E). In that solution, the density of farms at risk would be 0.078 (9 farms/114.42 sq km), the total area to be protected would represent 80.2% of the original area (114.42/142.5 sq km, i.e., savings equal to 19.8%), and the road density would be equal to 0.473 km of roads/ sq km (54.17 km/ 114.42 sq km). Such road density was twice higher than the road density shown by the original protection zone (0.47 vs. 0.22), and was even 10% higher (0.47 vs. 0.429 km/sq) than that of the smallest circle centered on one intersection (Fig. 2F).

Therefore, a control policy that addressed local bio-geographical conditions could be 19.8% less costly in terms of area coverage (e. g., control procedures could be implemented in one fifth less time or involve just 80.2% of the resources) and yet, it could be 23.8% more beneficial (0.078 farms at risk / sq km vs. 0.063 farms at risk/sq km in the ER protection zone, Fig. 2F).

Two findings rejected the hypothesis of homogeneous dissemination of farms at risk: (i) the ER-based protection zone did not reveal a similar number of farms per circle, and (ii) farms were, on average, 9.3 times closer to a highway or highway intersection than to one another (Supporting Materials). The data indicated that disease clusters (a network property) are not necessarily circular: ‘along-road’ clusters can also be found. A second network property (a Pareto-like distribution, Supporting Materials) was also observed (Chowell et al., 2008; Boisot and McKelvey, 2011). Therefore, network properties were documented even though the area under study (less than 115 sq km, in the optimal solution) was small. Findings were not unexpected: connectivity-based disease spread has been reported before (Rivas et al., 2003; Rivas et al. 2010).

It is suggested that protection zones can be more effective if connectivity is measured. The biological explanation for such statement resides in the fact that, for an exotic microbe to disseminate, it needs not only a susceptible host, but also a pre-existing connecting network (the microbe cannot build such network). Hence, protection zones may be chosen based on geographically explicit, cost-benefit analysis, which may consider estimates such as (i) number of sites at risk/sq km, (ii) total area to be protected, and (iii) proximity, continuity, and/or network length.

While ER circular protection zones may be a starting point when control policies are planned, such zones should be adjusted to meet the specific (bio-geographical) conditions of each epidemic. While, before geographical information systems emerged, control measures could not, rapidly, generate and process geo-referenced data, today such limitation no longer applies. CN-based protection zones could reduce time and resources spent on epidemic control.

References

- Andriani, P., and B. McKelvey, 2009: From Gaussian to Paretian Thinking: Causes and implications of power laws in organizations. *Organization Science* 20, 1053-1071.
- Aparicio, JP, and M. Pascual, 2007: Building epidemiological models from R_0 : an implicit treatment of transmission in networks. *Proc. R. Soc. B*, 274, 505–512.

- Barthélemy, M., 2011: Spatial networks. *Physics Reports* 499, 1–101.
- Boisot, M., and B. McKelvey, 2011: Connectivity, extremes, and adaptation: a power-law perspective of organizational effectiveness. *J. Management Inquiry* 20, 119–133.
- Chowell G., C. A. Torres, C. Munayco-Escate, L. Suárez-Ognio, R. López-Cruz, J.M. Hyman, and C. Castillo-Chavez, 2008. Spatial and temporal dynamics of dengue fever in Peru: 1994–2006. *Epid. Inf.* 136, 1667–1677.
- Cook, J. G., G. D. Cawley, and M. Richards, 2006: FMD and the contiguous cull. *Vet. Rec.* 159, 571-572.
- Cottam, E. M., J. Wadsworth, A. E. Shaw, R. J. Rowlands, L. G. Goatley, S. Maan, N. S. Maan, P. C. P. Mertens, K. Ebert, Y. Li, E. D. Ryan, N. Juleff, N. P. Ferris, J. W. Wilesmith, D., T. Haydon, D. P. King, D. J. Paton, and N. J. Knowles, 2008: Transmission pathways of Foot-and-Mouth Disease virus in the United Kingdom in 2007. *PLoS Pathogens* 4, e1000050.
- Dangerfield, C. E., J. V. Ross, and M. J. Keeling, 2009: Integrating stochasticity and network structure into an epidemic model. *J. R. Soc. Interface* 6, 761-774.
- Filipe, J. A. N., and M. M. Maule, 2004: Effects of dispersal mechanisms on spatio-temporal development of epidemics. *J. Theor. Biol.* 226, 125–141.
- Jewell, C. P., M. J. Keeling, and G. O. Roberts, 2009: Predicting undetected infections during the 2007 Foot-and-Mouth Disease outbreak. *J. R. Soc. Interface* 6, 1145-1151.
- Knight-Jones, T. J. D., J. Gibbens, J. M. Wooldridge, and K. D. C. Stark, 2011: Assessment of farm-level biosecurity measures after an outbreak of Avian Influenza in the United Kingdom. *Transbound. Emerg. Dis.* 58, 69–75.
- Lu, H., M. M. Ismail, O. A. Khan, Y. Al Hammad, S. S. A. Rhman, and M. H. Al-Blowi, 2010: Epidemic outbreaks, diagnostics, and control measures of the H5N1 highly pathogenic Avian Influenza in the Kingdom of Saudi Arabia, 2007–08. *Avian Dis.* 54, 350–356.
- Martinez-Lopez B., A. M. Perez, and J. M. Sanchez-Vizcaino, 2009: Social network analysis. Review of general concepts and use in preventive veterinary medicine. *Transb. Emerg. Dis.* 56:109–120.
- Rivas, A. L., G. Chowell, S. J. Schwager, F. O. Fasina, A. L. Hoogesteijn, S. D. Smith, S. P. R. Bisschop, and K. L. Anderson, 2010: Lessons from Nigeria: the role of roads in the geo-temporal progression of the avian influenza (H5N1). *Epid. Inf.* 138, 192-198.
- Rivas, A. L., S. Smith, P. J. Sullivan, B. Gardner, A. L. Hoogesteijn, and C. Castillo-Chávez, 2003: Identification of geographical factors associated with early epidemic spread of Foot-and-Mouth Disease. *Amer. J. Vet. Res.* 64, 1519-1527.
- Rivas, A. L., S. J. Schwager, S. Smith, and A. Magri, 2004: Early and cost-effective identification of high risk/priority control areas in foot-and mouth disease epidemics. *J. Vet. Med. B* 51, 263-271.
- Rivas, A. L., M. Chaffer, G. Chowell, D. Elad, O. Koren, S. D. Smith, and S. J. Schwager, 2008: Optimization of epidemiologic interventions: evaluation of spatial and non-spatial methods that identify Johne's Disease-infected subpopulations targeted to be intervened. *Isr. J. Vet. Med.* 63, 59-71.
- Ryan, E., J. Gloster, S. M. Reid, Y. Li, N. P. Ferris, R. Waters, N. Juleff, B. Charleston, B. Bankowski, S. Gubbins, J. W. Wilesmith, D. P. King, and D. J. Paton, 2008:

- Clinical and laboratory investigations of the outbreaks of foot-and-mouth disease in southern England in 2007. *Vet. Rec.* 163, 139-147.
- Thrusfield, M., L. Mansley, P. Dunlop, J. Taylor, A. Pawson, and L. Stringer, 2005: The foot--and-mouth disease epidemic in Dumfries and Galloway, 2001. 1: Characteristics and control. *Vet. Rec.* 156, 229-252.
- Thulke, H-H., D, Eisinger, and M. Beer, 2001: The role of movement restrictions and pre-emptive destruction in the emergency control strategy against CSF outbreaks in domestic pigs. *Prev. Vet. Med.* 99, 28-37.
- Watts, D. J., and S. H. Strogatz, 1998: Collective dynamics of 'small-world' networks. *Nature* 393, 440-442.
- Xie, F. and D. Levinson, 2007: Measuring the structure of road networks. *Geogr. Anal.* 39, 336-356.

Figure legends

Fig. 1. Features of the equal radius (ER) protection zone. **A:** protection and highway structure. **B:** Individual ER circles, centered on farms at risk. **C-E:** number of cases per circle, at selected circles. **F:** Farms at risk and highway intersections.

Fig. 2. Cost-benefit estimates of the ER and alternative protection zones. **A:** Case density in ER protection zone (0.063 cases/sq km, or 9/142.5 sq km). **B:** Road density in ER protection zone (0.22 km/sq km or 32.34 km/142.5 sq km). That corresponded to a ratio of 0.278 cases/km of roads (9/32.34 km). **C:** Case density in circles centered on a highway intersection were between: 0.144 cases/sq km (4/27.75, smaller circle), 0.102 (5/48.79, intermediate circle), and 0.056 (6/106.37 cases/sq km, larger circle, which partially fell outside the boundaries of the original protection zone). **D:** The apparent case density in the smallest polygon that included all farms at risks and was partially connected was 0.132 cases/sq km or 7/52.86). Only 7 of the 9 farms at risk were included because roads did not show a continuous (non-fragmented) connectivity: one road segment fell outside such polygon. **E:** The non-fragmented road length included in the smallest polygon was 26.28 km, which corresponded to a ratio of 0.266 cases/ km of roads (7/26.28 km) –a figure very close to the number of cases/km of road observed in the original protection zone, except that, in the small ‘along-road’ polygon the case density was twice higher (0.132 vs. 0.063 cases/sq km). **F:** If, instead, the surface of the region to be protected was expanded to include a highway intersection observed outside the south-east border of the original protection zone, all farms at risk would be included (100% or 7/7), case density would be 0.078 (9 cases/114.42 sq km), the total area to be protected would represent 80.2% of the original area (114.42/142.5 sq km, i.e., savings equal to 19.8%), and such solution would possess both a non-fragmented road structure and a road density equal to 0.473 km of roads/ sq km (54.17 km/ 114.42 sq km). Such road density was more than twice higher than the road density of the original protection zone (0.473/0.22=2.15). The control policy that addressed local bio-geographical conditions was (a) 19.8% less costly in terms of area coverage, and (b) 23.8% more beneficial (its number of farms at risk/sq km was 0.078 while that of ER zone was 0.063).

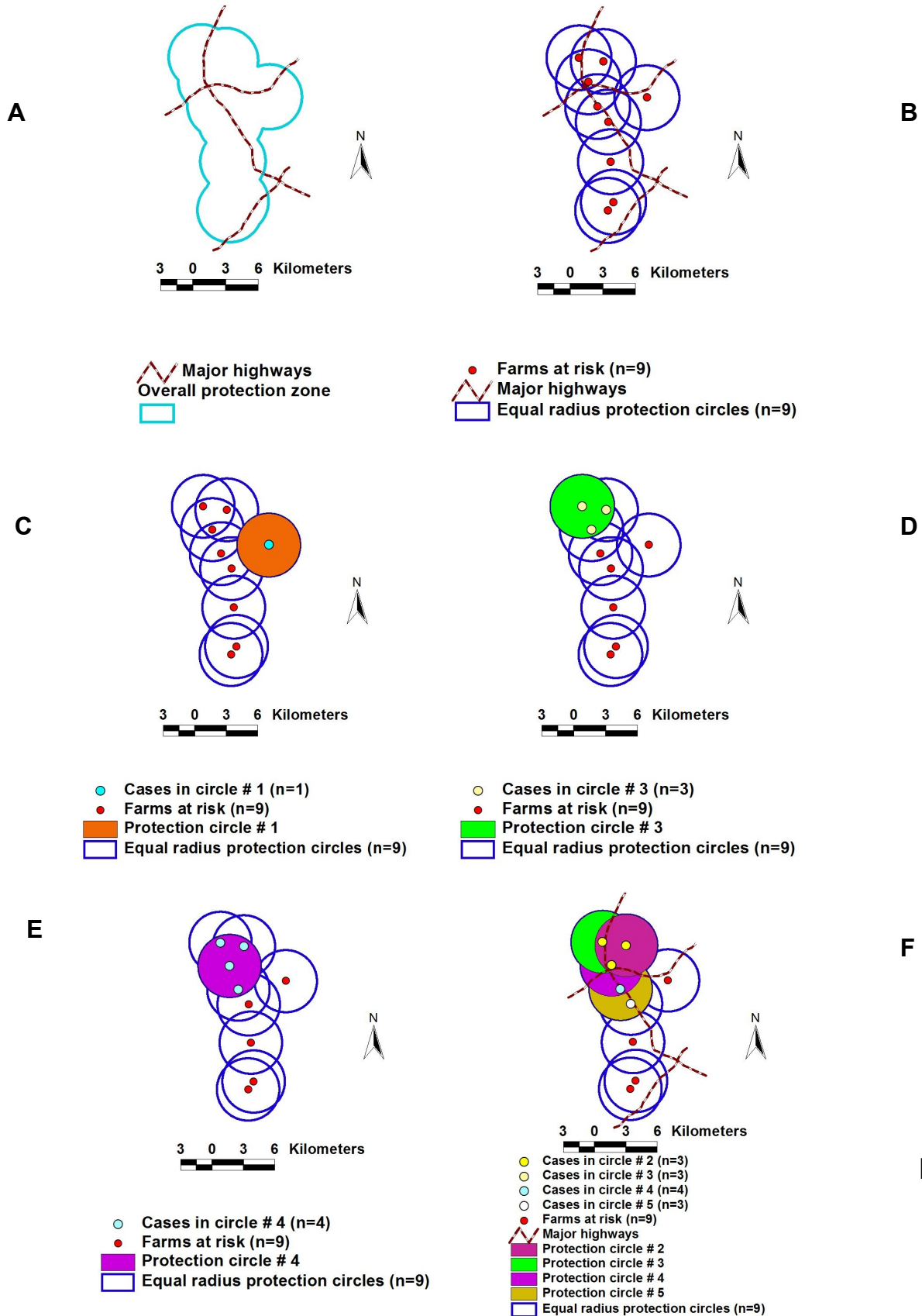


Fig. 1

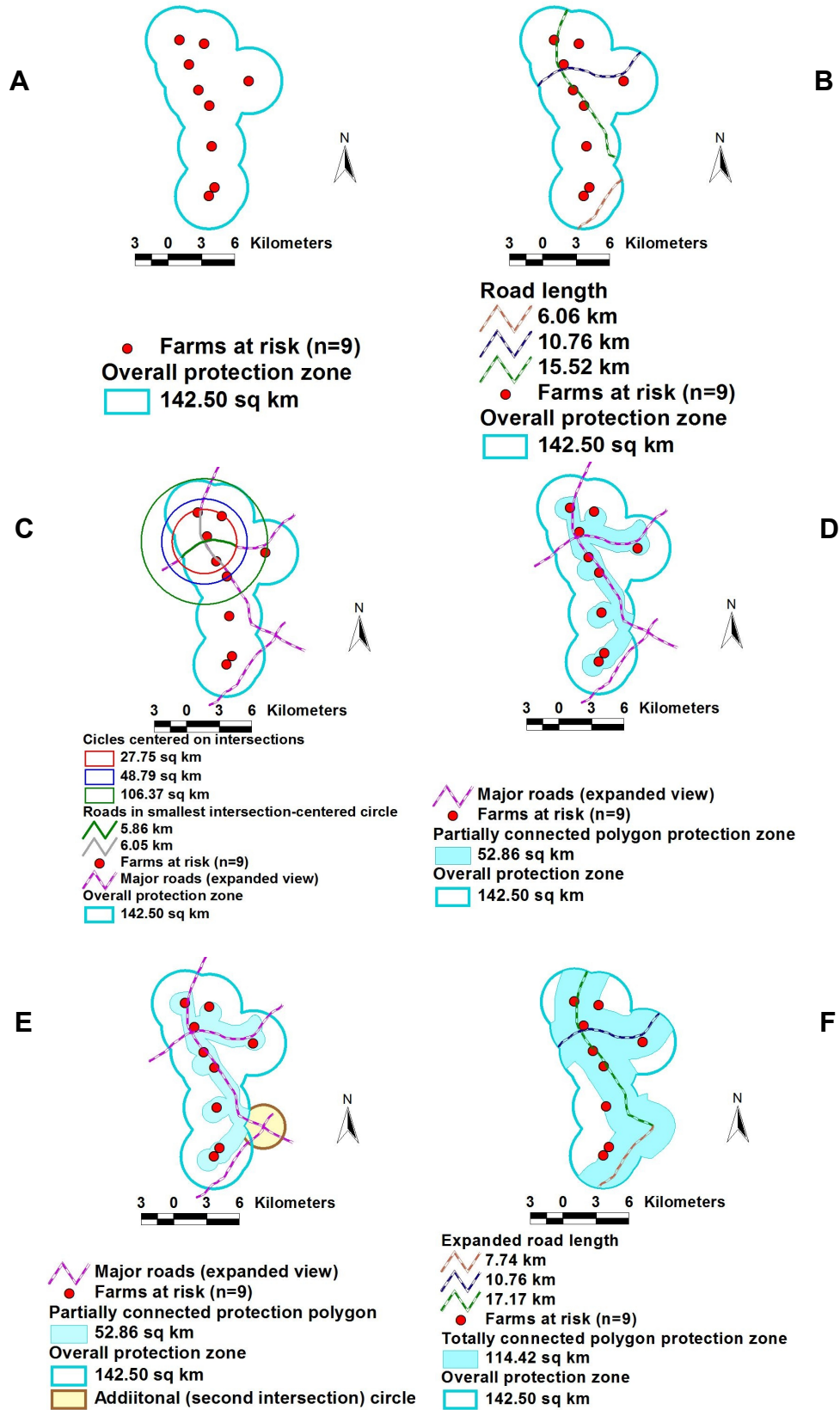


Fig. 2.

Supporting Materials

The process by which the geographic area under study was created is reported in Figs. 1 and 2. The number of farms at risk per equal radius (ER) circle is reported in Table I. Tables II and III report the Euclidean distance from each farm at risk to the nearest road or road intersection and the distance between farm pairs, respectively.

These data support the following three findings:

- (i) ER circles did not include a similar number of farms at risk: the median number of farms at risk per circle (generated by 9 farms distributed among 9 ER circles) was not 1: it was 2.5 ($P < 0.03$, Wilcoxon Signed Rank test, Table I), i.e., the homogeneous distribution of farms at risk (the justification for ER protection circles) was not justified;
- (ii) on average, farms at risk were 9.3 times closer to highways or highways intersections than to one another ($P < 0.01$, Tables II and III, and Fig. 3), i.e., farms at risk were not homogeneously distributed over space but clustered near to and along the road network (a network property); and
- (iii) the contribution of farms at risk per ER circle to the overall Chi square goodness-of-fit test showed a Pareto-like distribution (an additional network property): 11.1% of all ER circles (1/9) contributed 34.7% of the overall Chi square goodness-of-fit test (1.190/3.428, Fig. 4).

→ Request permission for publication to DEFRA defra.helpline@defra.gsi.gov.uk

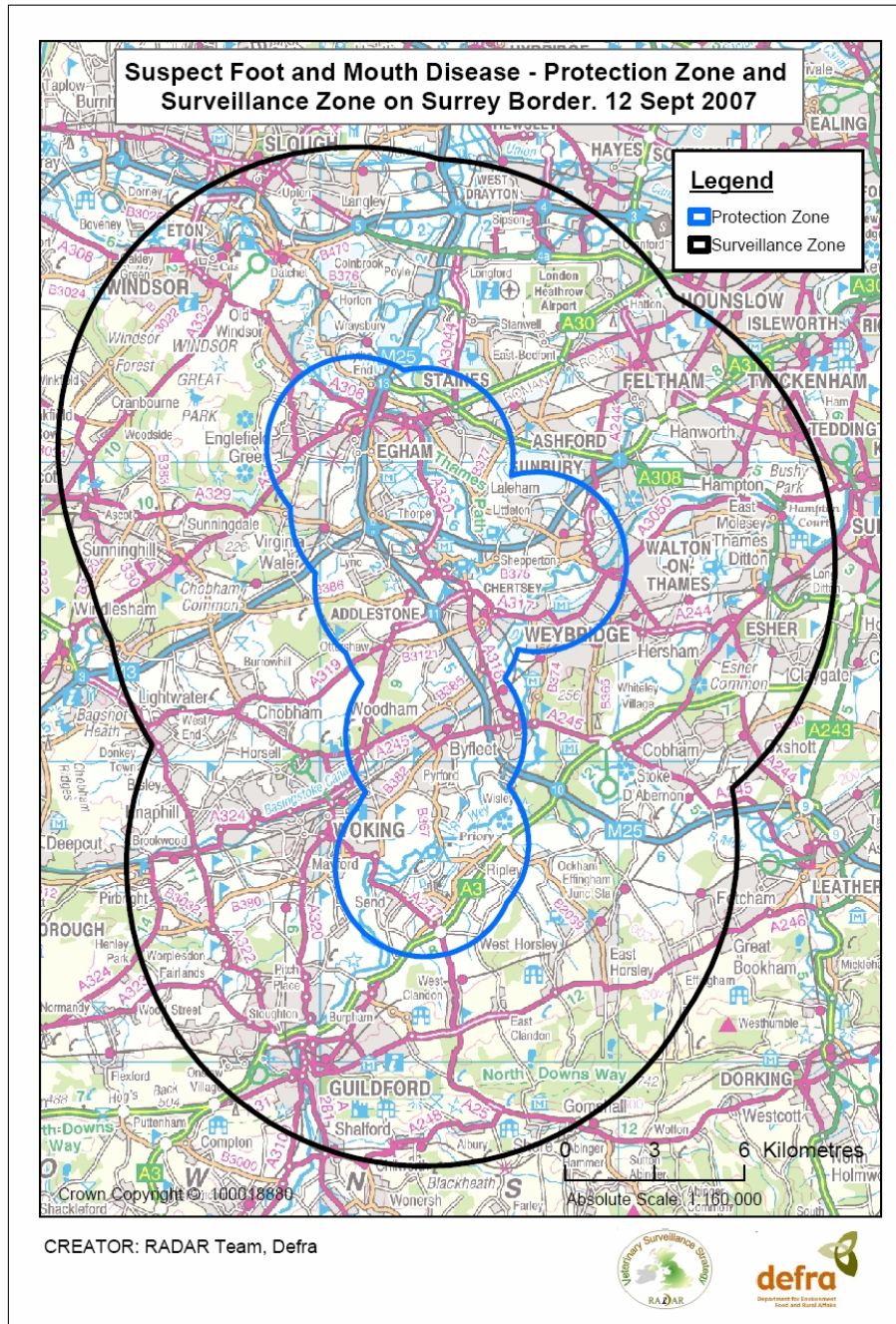
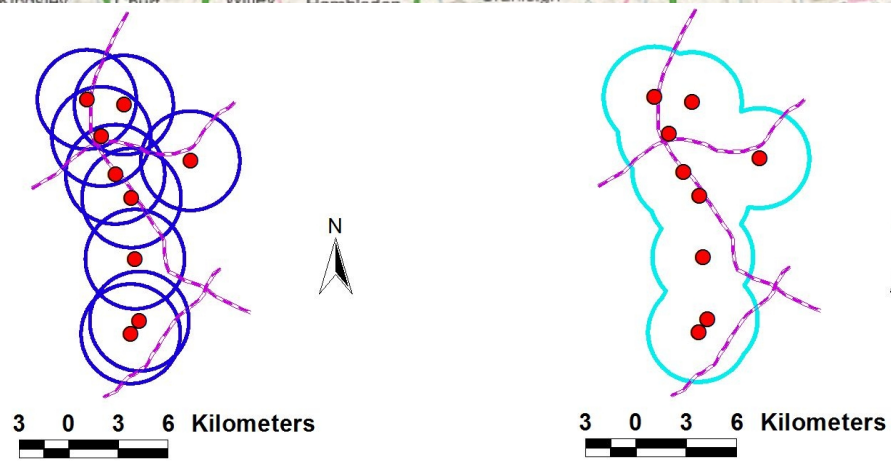
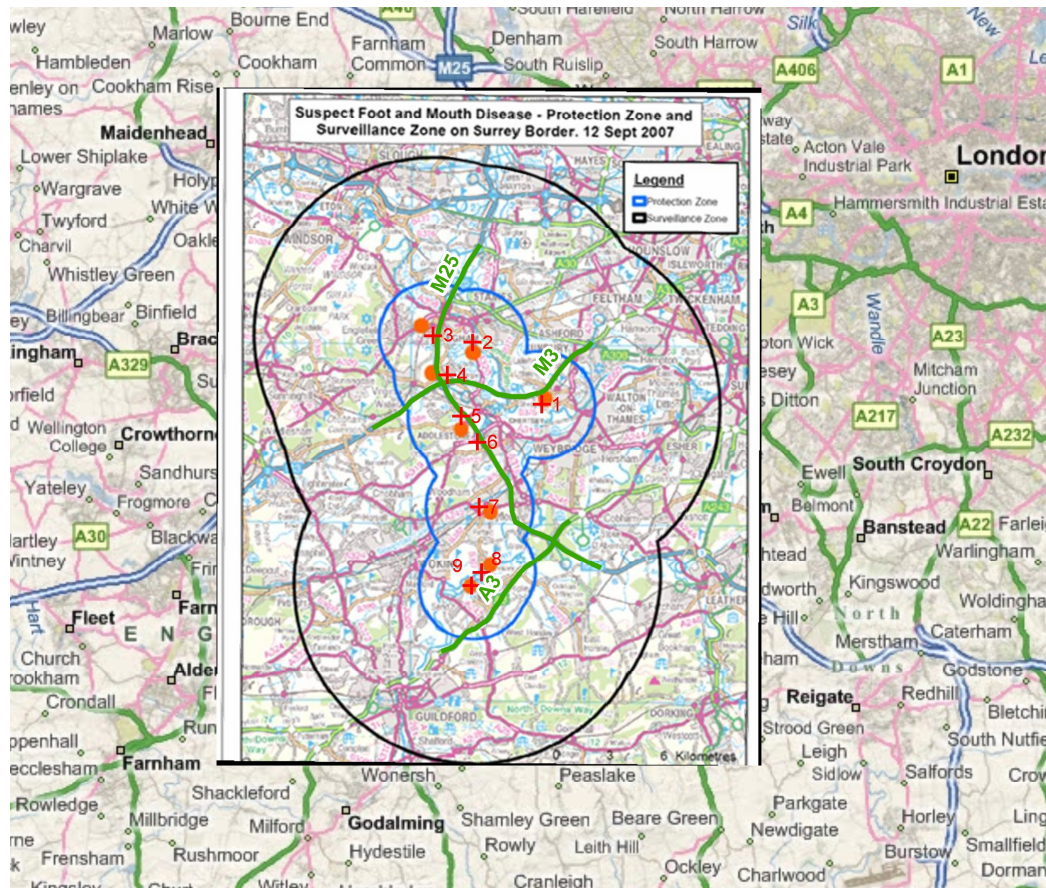


Fig. 1. DEFRA report and map, from 12 September, 2007, on a protection zone (blue polygon).




-  Farms at risk (n=9)
 Major roads (expanded view)
 ER protection circles (n=9)
-  Farms at risk (n=9)
 Major roads (expanded view)
 Overall protection zone

Fig. 2. Creation of a geo-referenced ‘protection zone’. **A:** An epidemic report (a JPG document, insert) was superimposed over a geo-referenced map, considering several points of road network as guides. **B:** Circles of various radii were created and empirically tested over the JPG map until segments of the new circles matched the perimeter of the sky blue polygon shown in the JPG file. The map displayed only shows the final solution, a set of 9 circles (“ER protection zones”) with their centroids (‘farms at risk’) indicated. **C:** By merging the 9 circles shown in B, the boundaries of the protection zone displayed in the original JPG map were recreated, as well as some segments of major highways.

Table I. Number of farms at risk per ER protection circle

Protection circle #	1	2	3	4	5	6	7	8	9
Farms at risk per circle	1	3	3	4	3	2	1	2	2

Table II. Farm distance to the nearest road or road intersection

	From farm #1	From farm #2	From farm #3	From farm #4	From farm #5	From farm #6	From farm #7	From farm #8	From farm #9
Distance (km) to the nearest road/road intersection	0.655	1.967	0.347	0.439	0.160	0.190	1.812	1.786	1.819
Median distance to nearest road or road intersection: 0.655 km									

Table III. Inter-farm distance

Distance (km) between farms at risk	farm # 1	farm # 2	farm # 3	farm # 4	farm # 5	farm # 6	farm # 7	farm # 8	farm # 9
farm # 1	*	5.1	7.2	5.8	4.5	4.1	6.8	10.1	11.1
farm # 2	5.1	*	2.5	2.3	3.9	5.6	9.1	12.9	13.8
farm # 3	7.2	2.5	*	2.5	4.9	6.5	10.1	13.7	14.5
farm # 4	5.8	2.3	2.5	*	2.4	4.2	7.7	11.3	12.0
farm # 5	4.5	3.9	4.9	2.4	*	1.8	5.5	8.9	9.6
farm # 6	4.1	5.6	6.5	4.2	1.8	*	3.5	7.4	8.1
farm # 7	6.8	9.1	10.1	7.7	5.5	3.5	*	3.8	4.5
farm # 8	10.1	12.9	13.7	11.3	8.9	7.4	3.8	*	0.9
farm # 9	11.1	13.8	14.5	12.0	9.6	8.1	4.5	0.9	*
Farm median inter-farm distance (km)	6.3	5.35	6.85	5	4.7	4.9	6.15	9.0	10.3
Global median inter-farm distance : 6.15 km									

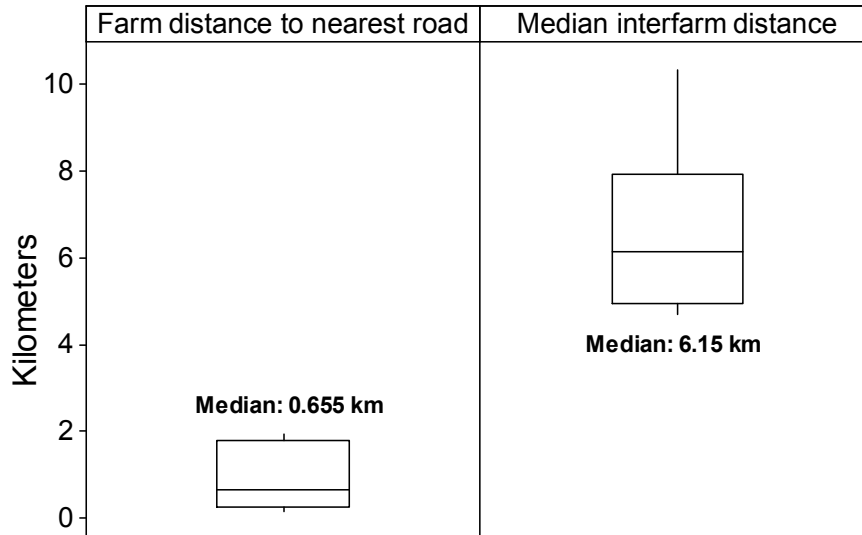


Fig.3. Distances between farms and between farms and the road network. The median farm inter-farm median distance (a median of medians) was 9.4 times greater than the median distance between farms at risk and the nearest road or road intersections ($P < 0.001$, Mann-Whitney test).

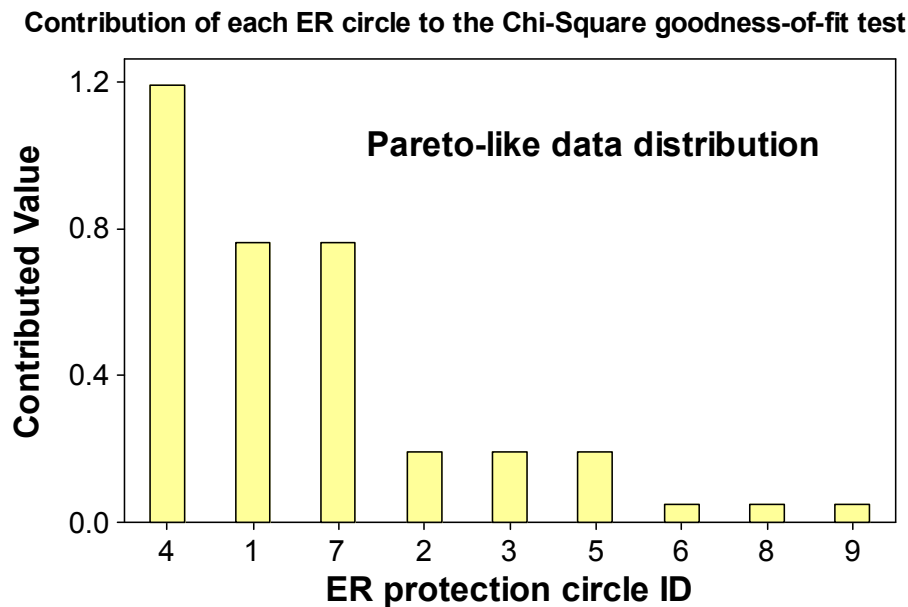


Fig. 4. Assessment of data trends. Circle #4 or 11.1% of all ER circles (1/9) contributed 34.7% of the overall Chi square goodness-of-fit test (1.190/3.428).